

FLUID BEHAVIOUR SIMULATION
Modelling of Water Diffusion in Ground Aircraft
De/Anti-icing Fluids for Numerical Prediction of
Laboratory Holdover Time

Prepared for

Transportation Development Centre

Safety and Security

Transport Canada

by

Anti-icing Materials International Laboratory (AMIL)

Université du Québec à Chicoutimi (UQAC)

October 1997

FLUID BEHAVIOUR SIMULATION
Modelling of Water Diffusion in Ground Aircraft
De/Anti-icing Fluids for Numerical Prediction of
Laboratory Holdover Time

by

Patrick Louchez

Alexandre Zouzou

Ling Liù

Rémi Sasseville

Anti-icing Materials International Laboratory (AMIL)

Université du Québec à Chicoutimi (UQAC)

October 1997

This report reflects the views of AMIL and not necessarily those of the Transportation Development Centre.

The Transportation Development Centre does not endorse products or manufacturers. Trade or manufacturers' names appear in this report only because they are essential to its objectives.

Un sommaire français se trouve avant la table des matières.



1. Transport Canada Publication No. TP 13113E		2. Project No. 9034 (DC 145)		3. Recipient's Catalogue No.	
4. Title and Subtitle Fluid Behaviour Simulation: Modelling of Water Diffusion in Ground Aircraft De/anti-icing Fluids for Numerical Prediction of Laboratory Holdover Time				5. Publication Date October 1997	
				6. Performing Organization Document No.	
7. Author(s) Patrick Louchez, Alexandre Zouzou, Ling Liù, and Rémi Sasseville				8. Transport Canada File No. ZCD1455-14	
9. Performing Organization Name and Address Laboratoire international des matériaux antigivre Université du Québec à Chicoutimi 555, boulevard de l'Université Chicoutimi, Québec G7H 2B1				10. PWGSC File No. XSD-6-01072	
				11. PWGSC or Transport Canada Contract No. T8200-6-6517	
12. Sponsoring Agency Name and Address Transportation Development Centre (TDC) 800 René Lévesque Blvd. West 6th Floor Montreal, Quebec H3B 1X9				13. Type of Publication and Period Covered Final	
				14. Project Officer Barry B. Myers	
15. Supplementary Notes (Funding programs, titles of related publications, etc.)					
16. Abstract <p>The present work investigates the introduction of a model for the water diffusion process to improve numerical simulation of the protection from icing provided by commercial Type I, Type II and Type IV de/anti-icing fluids used for aircraft on the ground.</p> <p>A specifically designed experimental method was established for the measurement of water diffusion in the fluids. The experimental set-up was calibrated and then validated against ethylene glycol. The water diffusion of commercial fluids and their dilution was measured at 23°C and 4°C. The diffusion coefficient reduction with temperature was shown to be in accordance with the variation predicted by the diffusion model. The water diffusion of ethylene glycol-based fluids was found slightly higher than that of propylene glycol-based fluids.</p> <p>The existing isothermal numerical model of the anti-icing performance tests used for de/anti-icing fluid certification was upgraded using the water diffusion model. Therefore, the code can now be proposed as a complement for the cold chamber testing for any type of fluid.</p>					
17. Key Words Aircraft de-icing fluid, WSET numerical simulation				18. Distribution Statement Limited number of copies available from the Transportation Development Centre	
19. Security Classification (of this publication) Unclassified	20. Security Classification (of this page) Unclassified	21. Declassification (date) —	22. No. of Pages xvi, 44, app.	23. Price —	



1. N° de la publication de Transports Canada TP 13113E		2. N° de l'étude 9034 (DC 145)		3. N° de catalogue du destinataire	
4. Titre et sous-titre Fluid Behaviour Simulation: Modelling of Water Diffusion in Ground Aircraft De/anti-icing Fluids for Numerical Prediction of Laboratory Holdover Time				5. Date de la publication Octobre 1997	
				6. N° de document de l'organisme exécutant	
7. Auteur(s) Patrick Louchez, Alexandre Zouzou, Ling Liù, et Rémi Sasseville				8. N° de dossier - Transports Canada ZCD1455-14	
9. Nom et adresse de l'organisme exécutant Laboratoire international des matériaux antigivre Université du Québec à Chicoutimi 555, boulevard de l'Université Chicoutimi, Québec G7H 2B1				10. N° de dossier - TPSGC XSD-6-01072	
				11. N° de contrat - TPSGC ou Transports Canada T8200-6-6517	
12. Nom et adresse de l'organisme parrain Centre de développement des transports (CDT) 800, boul. René-Lévesque Ouest 6^e étage Montréal (Québec) H3B 1X9				13. Genre de publication et période visée Final	
				14. Agent de projet Barry B. Myers	
15. Remarques additionnelles (programmes de financement, titres de publications connexes, etc.)					
16. Résumé <p>Le travail présenté propose un modèle du processus de diffusion de l'eau afin d'améliorer la simulation numérique de la protection contre le gel, fournie par les fluides dé/antigivrant commerciaux de Type I, Type II et Type IV utilisés pour les avions au sol.</p> <p>Une méthode expérimentale, conçue spécialement, a été établie pour la mesure de la diffusion de l'eau dans les fluides. Le montage expérimental a été calibré puis validé à l'aide de l'éthylène glycol (EG). La diffusion de l'eau dans les fluides commerciaux et leurs dilutions a été mesurée à 23 °C et 4 °C. La réduction du coefficient de diffusion en fonction de la température est en accord avec la variation prédite par le modèle de diffusion. La diffusion des fluides de base EG s'est avérée légèrement plus élevée que celle des fluides de base propylène glycol (PG).</p> <p>Le modèle numérique isotherme existant simulant les tests de performance anti-givre utilisés pour la certification des produits dé/antigivrant a été amélioré en introduisant le modèle de diffusion de l'eau. En conséquence, le code peut maintenant être proposé comme complément aux essais en chambre froide.</p>					
17. Mots clés Fluide dégivrant pour avion, simulation numérique WSET			18. Diffusion Le Centre de développement des transports dispose d'un nombre limité d'exemplaires.		
19. Classification de sécurité (de cette publication) Non classifiée	20. Classification de sécurité (de cette page) Non classifiée	21. Déclassification (date) —	22. Nombre de pages xvi, 44, ann.	23. Prix —	

AMIL PROJECT TEAM

Louchez P. R., Ph.D., Eng.: Project Director

Laforte J.L., D.Sc., Eng.: Senior Adviser

Bernardin S., M.Sc.: AMIL Manager

Ling L., M. Sc.: Chemist

Sasseville R., B. Sc.: Research Assistant

Zouzou A., B. Sc.: Computer Analyst

Perron E., M.Sc., Eng.: Mechanical Engineer

Tremblay M., M. Sc., Eng.: Chemical Engineer

He Z., M. Sc.: Research Assistant

Nguyen-Dang Du: Research Assistant

ACKNOWLEDGEMENTS

The de/anti-icing fluids were graciously provided by their respective manufacturers: ARCO Chemicals, HOECHST, OCTAGON PROCESS, UNION CARBIDE and SPCA. The authors are indebted to Mrs. S. Bernardin as well as Mr. Z. He for managing all questions regarding fluids. The technical assistance of Mr. C. Paquin-Lavigne, Mr. S. Jomphe and Mr. A. Barette with the experimental set-up was also much appreciated.

SUMMARY

Considering the limitation of the information gathered from the experimental testing of ground aircraft de/anti-icing fluids, Transport Canada funded a research project to develop a numerical simulation of the laboratory holdover time evaluation procedures. The resulting model represented fairly well the physical processes, and it was validated for Type I and Type II fluids. However, due to the crude modelling of the water diffusion coefficient, the simulation could not be considered as equivalent to the experimental situation, especially in the case of Type IV fluids. The objective of the present work was to develop a model of the water diffusion process in de/anti-icing fluids to improve the numerical simulation of the protection against ice formation provided by commercial Type I, Type II and Type IV fluids, particularly under Water Spray Endurance Test (WSET) conditions.

The experimental method chosen for the measurement of water diffusion of de/anti-icing fluids is a column free diffusion technique. Glass tubes were specifically designed for the tests, and were fitted with a sintered glass ring to minimise instability at the test fluid to water interface. The diffusion coefficient is calculated from Fick's second law by measuring the initial and final concentration of the fluid at a specific position in the tube after a prescribed period of time. The fluid water concentration is determined by a refractive index method.

The experimental set-up was calibrated against 50% ethylene glycol (EG)-water system and then validated against the EG 75%-water system. It was found that the experimental apparatus was capable of providing reproducible results with a $\pm 5\%$ accuracy. The water diffusion of commercial fluids and their dilution (75%, 50%, 25%) were measured at 23°C and 4°C. It was found that, for all the fluids, the diffusion coefficient, D , is considerably reduced at 4°C compared to that at 23°C. This reduction was shown to be in accordance with the viscosity, μ , and temperature, T , variation as predicted by the diffusion model which assumes that, at a given concentration, the product $D \mu / T$ is constant. The diffusion coefficient value was shown to increase with the diminution of the fluid concentration. The water diffusion

of EG and the EG-based fluids was found slightly higher than those of PG and the PG-based fluids at all concentration levels.

The isothermal numerical model of the WSET situation was upgraded using the water diffusion model. A very good agreement was found, for all fluid types, between numerical and experimental holdover time. Consequently, the code can now be proposed as a complement for the WSET cold chamber testing. To simulate other laboratory tests or outdoor conditions, it is recommended to upgrade the model by incorporating thermal effects.

SOMMAIRE

Considérant les limitations de l'information accumulée au cours des essais expérimentaux sur les fluides dé/antigivrant utilisés pour les avions, Transports Canada a financé un projet de recherche pour développer une simulation numérique des procédures d'évaluation de temps de tenue en laboratoire. Le modèle résultant représentait assez bien le processus physique et a été validé pour les fluides de Type I et II. Cependant, en raison de la modélisation sommaire du coefficient de diffusion de l'eau, la simulation ne pouvait être considérée comme équivalente à la situation expérimentale, particulièrement dans le cas des produits de Type IV. L'objectif du présent travail était de développer un modèle du processus de diffusion de l'eau dans les fluides dé/antigivrant pour améliorer la simulation numérique de la protection contre la formation de glace, fournie par les fluides commerciaux de Type I, Type II et Type IV, particulièrement sous conditions de l'essai normalisé d'endurance sous précipitation givrante (WSET).

La méthode expérimentale choisie pour la mesure de la diffusion de l'eau dans les fluides dé/antigivrant est une technique de diffusion libre en colonne. Des tubes à essai ont été conçus spécialement pour les essais et sont sertis d'anneaux de verre poreux pour minimiser l'instabilité à l'interface du fluide dégivrant et de l'eau. Le coefficient de diffusion est calculé à partir de la deuxième loi de Fick en mesurant la concentration initiale et finale du fluide à une hauteur spécifique dans le tube après une période de temps prédéterminée. La concentration en eau dans le fluide est obtenue par une méthode d'indice de réfraction.

Le montage expérimental a été calibré par le système eau-éthylène glycol (EG) à 50 % puis validé par le système eau-éthylène glycol (EG) à 75 %. Il a été démontré que l'appareil expérimental était capable de fournir des résultats reproductibles avec une précision de $\pm 5\%$. La diffusion de l'eau dans les fluides commerciaux et leurs dilutions (75 %, 50 %, 25 %) a été mesurée à 23 °C et 4 °C. Les résultats ont montré, pour tous les fluides, que le coefficient de diffusion D est considérablement réduit à 4 °C par rapport à 23 °C. Cette réduction s'est avérée être en accord avec la variation

de viscosité, μ , et de température, T, telle que prédite par le modèle de diffusion qui suppose que, à une concentration donnée, le produit $D \mu / T$ est constant. La valeur du coefficient de diffusion s'accroît avec la diminution de la concentration en fluide. La diffusion de EG et des fluides de base EG s'est avérée légèrement plus élevée que celle de PG et des fluides de base PG à tous niveaux de concentration.

Le modèle numérique isotherme de la situation du WSET a été amélioré en utilisant le modèle de diffusion de l'eau. Un très bon accord a été trouvé, pour tous les types de fluides, entre les temps de tenue (HOT) numériques et expérimentaux. En conséquence, le code peut maintenant être proposé comme complément aux essais en chambre froide. Afin de simuler d'autres conditions d'essais en laboratoire ou à l'extérieur, il est recommandé d'améliorer le modèle en incluant les effets thermiques.

TABLE OF CONTENTS

1. INTRODUCTION.....	1
1.1 Background.....	1
1.1.1 De-icing and Anti-icing Procedures	1
1.1.2 Holdover Time.....	2
1.1.3 Water Diffusion	3
1.1.4 Numerical Modelling.....	3
1.2 Objectives.....	4
2. MODELLING OF WATER DIFFUSION.....	5
2.1 Principles of Liquid Diffusion	5
2.2 Theoretical Molecular Ratio.....	6
3. EXPERIMENTAL METHODOLOGY.....	9
3.1 Measurement of Liquid Diffusion Coefficients.....	9
3.2 Experimental Apparatus	10
3.3 Experimental Procedure.....	13
3.4 Concentration Measurement Method	14
3.5 Diffusion Calculation Method	17
3.6 Calibration of the Method	18
3.7 Validation of the Method	20
4. WATER DIFFUSION RESULTS AND DISCUSSION	23
4.1 Tested De-icing and Anti-icing Fluids	23
4.2 Diffusion Results.....	24
4.3 Estimated Diffusion Coefficient and Molecular Ratio Results	28
5. NUMERICAL SIMULATION.....	31

5.1 Descriptions of WSET and HHET Simulations.....	31
5.2 Governing Equations	32
5.3 Calculation Strategy.....	33
5.4 Numerical Results.....	35
6. CONCLUSIONS	39
REFERENCES.....	43
APPENDIX A: FLUID PROPERTIES	

LIST OF TABLES

TABLE 1: REFRACTIVE INDEX CURVE-FIT FOR ETHYLENE GLYCOL AND PROPYLENE GLYCOL.....	15
TABLE 2: SERIES A TUBES CALIBRATION	19
TABLE 3: SERIES B TUBES CALIBRATION	19
TABLE 4: VALIDATION EXPERIMENTS WITH ETHYLENE GLYCOL (75% AT 23°C).....	20
TABLE 5: DIFFUSION COEFFICIENT FOR ETHYLENE GLYCOL	21
TABLE 6: DIFFUSION COEFFICIENT FOR PROPYLENE GLYCOL.....	22
TABLE 7: DE-ICING AND ANTI-ICING FLUID DEFINITION.....	23
TABLE 8: FLUID REFRACTIVE INDEX CURVE-FIT COEFFICIENTS	24
TABLE 9: TYPICAL FLUID EXPERIMENTS RESULTS.....	25

LIST OF FIGURES

FIGURE 1: MOLECULAR RATIO FOR ETHYLENE GLYCOL IN WATER.....	7
FIGURE 2: MOLECULAR RATIO FOR PROPYLENE GLYCOL IN WATER.....	8
FIGURE 3: MENISCUS ON GLASS SURFACE	11
FIGURE 4: WATER DIFFUSION MEASUREMENT APPARATUS.....	12
FIGURE 5: GLASS TUBE SET-UP.....	13
FIGURE 6: ETHYLENE AND PROPYLENE GLYCOL CONCENTRATION VS REFRACTIVE INDEX.....	16
FIGURE 7: CALIBRATION OF DIFFUSION WITH ETHYLENE GLYCOL	19
FIGURE 8: TYPE I FLUIDS DIFFUSION COEFFICIENTS	26
FIGURE 9: TYPE II FLUID DIFFUSION COEFFICIENTS	27
FIGURE 10: TYPE IV FLUID DIFFUSION COEFFICIENTS.....	27
FIGURE 11: PROBLEM SCHEMATICS	31
FIGURE 12: VALIDATION OF HOT IN WSET	35
FIGURE 13: VALIDATION OF HOT IN HHET	36
FIGURE 14: WATER DIFFUSION EFFECT.....	37

NOMENCLATURE

g	gravitational acceleration (m^2/s)
h	fluid height (mm)
i	refractive index (-)
k	Boltzmann constant (J/K)
l	liquid height (mm)
m''	mass transfer rate (kg/s)
n	power factor (-)
t	time (s)
x	downstream distance along the plate (mm)
y	vertical height normal to the plate (mm)
C	fluid concentration (-)
D	coefficient of water diffusion (m^2/s)
D^*	estimated coefficient of water diffusion (m^2/s)
T	temperature (K)
R_m	molecular ratio (-)
$\dot{\gamma}$	shear rate (1/s)
μ	dynamic viscosity (Pa.s)
θ	plate angle (degrees)
ρ	density (kg/m^3)
σ	surface tension (N/m)
τ	shear stress (Pa)

Indices

ls	low shear
w	water
zs	zero shear
0	initial condition

Acronyms

EG	ethylene glycol
FFT	first freezing time
FIE	first icing event
HHET	high humidity endurance test
HOT	holdover time
MIT	mean icing time
PG	propylene glycol
WSET	water spray endurance test

1. INTRODUCTION

1.1 Background

1.1.1 De-icing and Anti-icing Procedures

At airports, de-icing procedures are used to remove all forms of ice while the aircraft is on the ground waiting for takeoff. In the course of the last twenty years, the use of specifically formulated mixtures of water and glycol, called de-icing fluids, has been gradually introduced. These mixtures are now defined by standard material specifications and denominated Type I fluids (AMS #1424, 1993). According to these specifications, neat Type I fluids are Newtonian, containing at least 80% of glycol. The latest revision of AMS #1424 (AMS #1424b, 1997) does not require Type I fluids to be Newtonian, but most of the commercial fluids have this characteristic.

Anti-icing procedure is used to prevent formation of ice. Anti-icing fluids are much more viscous than de-icing fluids as a result of the introduction of large-polymer molecules to the water-glycol solution. However, a pseudo-plastic behaviour is also required since the fluid viscosity has to be markedly shear stress dependent, in order to ease the fluid flow-off during the take-off run. Anti-icing fluids are now defined by standard material specifications and denominated Type II fluids (AMS 1428, 1993). According to these specifications, Type II fluids are pseudo-plastic, containing about 50% of glycol.

As queuing time between gate and runway becomes larger with increasing airport traffic, the need for extended protection time has prompted the development of a new generation of anti-icing fluids, now defined by standard material specifications and denominated Type IV fluids (AMS 1428b, 1997).

1.1.2 Holdover Time

Holdover Time (HOT) is the time anti-icing fluid will prevent the formation of frozen contamination on the protected surfaces of an aircraft. Laboratory HOT are evaluated in standardised cold chamber precipitation simulations. These experimental simulations are performed to rate the protection performance of commercial de/anti-icing fluids as Type I, II, III or IV. The resulting experimental HOT are also used, along with outdoor testing, to estimate the expected HOT available for de-icing/anti-icing operations under actual natural weather conditions. These expected HOT are listed in guideline tables for airline pilots and ground operators.

The present study focuses on the laboratory HOT since modelling the specific laboratory situation is a necessary first step before attempting to reproduce all weather conditions which are covered in service HOT tables. Two experimental procedures, performed by the Anti-Icing Materials International Laboratory (AMIL), provide performance assessment of the ice holdover time of the fluids: the Water Spray Endurance Test (WSET) and the High Humidity Endurance Test (HHET), (Laforte 1990; Laforte 1992). The WSET reproduces a freezing fog at -5°C and $5 \text{ g/dm}^2\text{h}$ and the HHET a hoar-frost at 0°C and $0.3 \text{ g/dm}^2\text{h}$. These laboratory simulations are performed by testing products poured on polished, 30 cm long, flat, inclined, aluminium plates. The inclination is taken at 10 degrees as the most severe case for the draining process, since actual wing surface angles are generally smaller than 10 degrees.

For fluid certification, the minimum WSET holdover time required is three minutes for Type I fluids, 30 minutes for Type II fluids, and 80 minutes for Type IV fluids, while the minimum HHET holdover time required is 20 minutes for Type I fluids, 240 minutes for Type II fluids, and 480 minutes for Type IV fluids.

1.1.3 Water Diffusion

The water diffusion is the physical property accounting for all the transport of water molecules through the fluid mixture. All the certified, commercial anti-icing and de-icing fluids are based on ethylene glycol (EG) or propylene glycol (PG) due to the EG and PG property of lowering the freezing point of water (Curme, 1952). The water diffusion of the fluids is defined as an important parameter used to assess the water penetration properties of the fluid which may affect its ice holdover time under sub-zero precipitation conditions. Water penetration dilutes the liquid concentration and thus increases the freezing point, but it also decreases the viscosity of the fluid and accelerates the draining and thinning of the fluid on the inclined aircraft surface. The water diffusion coefficient is one of the indispensable parameters in the development of numerical modelling to predict the duration of the protection provided by a given fluid under given precipitation conditions (Louchez, 1996).

1.1.4 Numerical Modelling

The need to better understand the governing mechanisms of the failure process has prompted Transport Canada to support a research program to investigate the freezing mechanism of de/anti-icing fluids under cold precipitation, with a particular emphasis on the dilution mechanism. In phase I of this program, an isothermal model was developed reproducing the WSET and HHET conditions (Louchez, 1996). This model considers that air, fluid and plate remain constantly at the same temperature (-5°C for WSET). The diffusion process was only crudely represented by a constant diffusion coefficient based on equivalent EG content, even for PG based fluids. Results were found slightly but significantly different than the experimental situation so that it could not be considered as equivalent to the laboratory certification procedure. Also, the diffusion of Type IV products was not correctly simulated.

1.2 Objectives

The general objective of the work covered by this report is to improve the existing numerical simulation predicting the duration of protection provided by a given fluid, of known characteristics, in a given precipitation condition, by developing a model for the process of diffusion of precipitation water into the fluid.

The specific objective of the present phase II of the program is to extend the validity of the simulation to Type IV fluids. This work thus essentially focuses on the water diffusion coefficient in de/anti-icing fluids. The experimental aspect provides measurements of the diffusion coefficient of water into de-icing and anti-icing fluids at four concentrations: (neat fluid) 100%, 75%, 50% and 25% and two temperatures (23°C and 4°C). The numerical aspect establishes a calculation model for this parameter at all temperatures, concentrations and shear rates relevant to the actual protection process and provides a comparison with the laboratory testing procedures WSET and HHET for Type I, II and IV fluids.

2. MODELLING OF WATER DIFFUSION

2.1 Principles of Liquid Diffusion

A simple approach to the description of the diffusion process in a liquid is to consider that, as in the crystal lattice of a solid, holes exist and their number depends on the temperature. Mass diffusion thus occurs as molecules are moving from holes to holes. If all molecules are identical, then the phenomenon is known as self-diffusion. Although it is possible to observe this process by radioactive marking of the particles, there is no net transport of anything. However, there is transport of heat or momentum when self-diffusion is driven by temperature or velocity gradients. The situation of interest here is the mutual or binary diffusion process where two different components are in presence, one considered as solvent, the other as solute. The random molecular motion tends to uniformly distribute the solute into the solvent. Therefore, at a given time when the homogeneous state is not yet achieved, there is a net transport of the solute, m'' (kg / m² s), which is proportional to the gradient of concentration, C (kg/kg), according to Fick's first law given in Equation 1 for the one-dimensional case along the y axis. The coefficient of proportionality is known as the coefficient of diffusion D (m² / s) (Sherwood, 1975).

$$m'' = -D \frac{\partial C}{\partial y}$$

Equation 1: Diffusion Flux

2.2 Theoretical Molecular Ratio

From the analysis of existing work (Johnson and Babb, 1956), the theoretical calculation of D can be performed by determining the diffusion coefficient as a function of the dynamic viscosity of the solvent, μ , and temperature T . The resulting formula can be expressed as shown in Equation 2, where r_0 (m) is the solute molecular radius (taken at $2.03 \cdot 10^{-10}$ m for water) and k is the Boltzmann constant ($1.38 \cdot 10^{-23}$ J/K).

$$D = \frac{k T}{6\pi Rm \mu r_0}$$

Equation 2: Theoretical Prediction for D

This calculation requires the evaluation of a dimensionless parameter, called here the molecular ratio and denoted Rm , which is related to the ratio of molecular sizes between solvent and solute. The relationship between Rm and the ratio of molecular sizes is through the ratio of enthalpies of vaporization and molecular weight (Sherwood, 1975). There is no general theory but since the number Rm is related to the molecular sizes of mixture and solute, it only depends on concentration. For the extreme case of mixture of a very large molecule solute into a solvent of small molecules, Rm is exactly equal to **one**, according to Stokes-Einstein's hydrodynamic theory (Einstein, 1905), but it is much reduced for the case of a very small molecule solute into a solvent of large molecules according to Garner and Marchant's results (1961). The case where the solute and solvent molecules are identical corresponds to the self-diffusion process; according to Eyring's kinetic theory (Jost, 1965), its theoretical value is equal to $1/(3\pi)$. For intermediate cases, relatively small molecules diffusing in mixtures of larger

molecules such as water in anti-icing fluid, there is no theoretical prediction for R_m .

To assess the above assumption, the molecular ratio has to be calculated and shown to be independent of temperature at a given concentration. The amount of existing results for fluids pertinent to de-icing and anti-icing procedures is restricted to measurements of EG/water and PG/water systems. Garner and Marchant (1961) and Byers and King (1966) have produced the most detailed results, providing D value for EG at various concentrations for temperatures between 20 °C and 40 °C. The result of processing their data, using viscosity data (Curme 1952), is given in Figure 1 for EG and in Figure 2 for PG. It can be seen that R_m is fairly constant at a given concentration, when the temperature varies. With increasing concentration level of glycol in the mixture, R_m decreases, and, correspondingly, the diffusion coefficient increases.

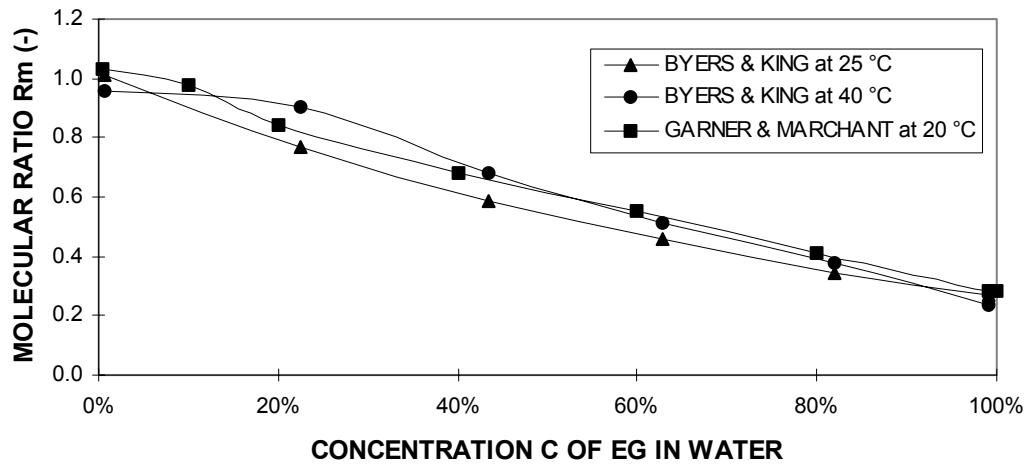


Figure 1: Molecular Ratio for Ethylene Glycol in water

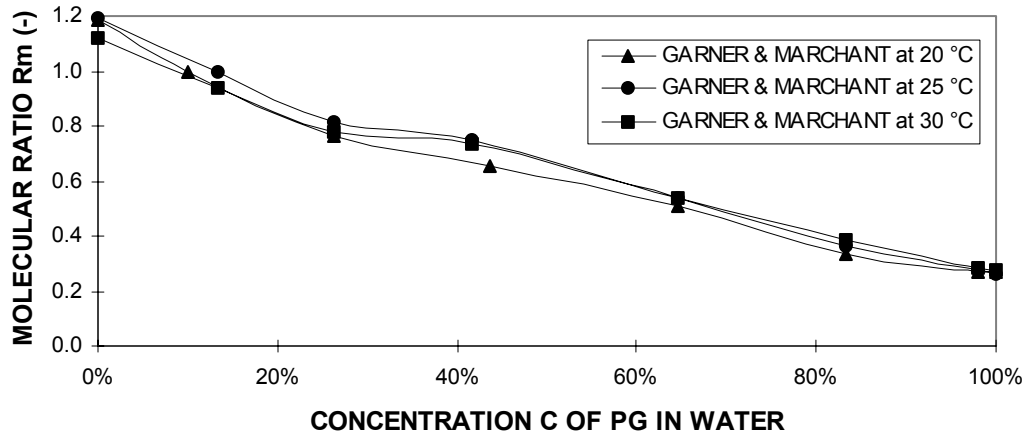


Figure 2: Molecular Ratio for Propylene Glycol in water

For de-icing fluids, the average molecular size of the diluted fluid with respect to that of water varies from 2 to 1 as dilution increases. Comparing with similar size combination, the dimensionless number R_m for de-icing fluids should be between 0.1 and 1. For anti-icing fluids, the average molecular size of the fluid may be significantly modified by the presence of the large polymers used as thickening agents and, consequently, values much lower than 0.1 are expected for R_m .

Although R_m is not a universal constant, it is still of practical interest. First, the measurement at a given temperature can be translated to another temperature given the knowledge of the viscosity at both temperature. This is a fortunate feature since the variation of the viscosity of de-icing and anti-icing fluids is well documented between -25°C and 20°C by the AMIL certification measurements. Secondly, the anti-icing fluids are pseudo-plastic, therefore it is expected that not only viscosity but also all molecular diffusion properties are dependent on shear stress. Since all measurement methods of D are restricted to zero shear conditions, Equation 2 is the only means to estimate D at a given shear stress.

3. EXPERIMENTAL METHODOLOGY

3.1 Measurement of Liquid Diffusion Coefficients

The available experimental techniques to measure the diffusion coefficient, D , could be classified as either free, restricted or steady-state diffusion (Hung, 1976). Free diffusion takes place in an interface of two liquid phases in a vertical column and may continue until concentration changes begin to occur at the ends of the column. Restricted diffusion differs from free diffusion in that the duration of the experiment is sufficiently long to allow appreciable concentration changes at the ends of the column. A true steady state diffusion requires constant concentration at both ends of the column. Among these experimental methods, interferometric methods (free diffusion) and diaphragm cell methods (steady-state diffusion) have proven more popular than others due to their accuracy (Tyrrell, 1961). The concentration distribution could be determined continuously or at intervals throughout the experiment by using these methods. The main disadvantages with these methods include the costly and elaborate equipment which is hard to duplicate and operate, the complexity in data analysis, and the difficulty to popularize for routine industrial tests.

The AMIL method is a free diffusion method. In this type of method, the initial concentration distribution is known and the concentration distribution at the end of the experiment can also be determined. The water diffusion can be calculated by using Fick's second law, thus providing the concentration distribution as a continuous function of distance and time. To keep simple analytical solutions, all methods used in these techniques are based on a simple initial composition, usually that of a uniform initial concentration C_0 . At the end of the experiment, either the concentration distribution or the amount of material at various positions in the column must be measured. Many of these techniques thus allow a standard type of analysis to be made of samples removed from the system, but this simplicity is usually achieved at some expense in accuracy.

The AMIL method uses a sample removal technique. The initial concentration of the fluid and its final concentration at a fixed position in the column are determined by refractive index. The interest of AMIL method resides in the low cost design of the experimental apparatus. Its accuracy and reliability is obtained by the combination of simple operational procedures and a specifically written software for the data analysis. The method could be easily introduced to the manufacturers of anti-icing and de-icing fluids for the routine tests of their products.

The measurements of Garner & Marchant and Byers & King, as well as others, generally differ by 5% up to 10%. This is the order of accuracy which can be reliably attributed to D values, even when experimental set-up are repetitive between 1% and 3% (Johnson & Babb, 1956).

3.2 Experimental Apparatus

In the free diffusion technique, the challenge is to procure a stable initial interface between both liquids. In most cases, there is a significant difference in the energy between air/fluid/glass interface and fluid/fluid/glass interface. In the case of glycol-based fluid and water, the fluid/fluid/glass interface has a much lower free energy. The excess is thus released in turbulent motions during the establishment of the interface. Regardless of the care taken to “deposit” the second fluid on top of the first one, large vortices are generated producing fluid engulfments which modify significantly and erratically the initial concentration. Therefore, this reduces the subsequent analysis of the concentration-time variation since it precludes the use of the one-dimensional diffusion equation to predict the water diffusion value. This phenomenon can also be described as a consequence of the difference in surface tensions. The water surface tension being about twice as large as that of de/anti-icing fluid, the meniscus of the fluid alone, which is upward, must transform into a downward meniscus when the water is present (Figure 3).

To avoid this initial instability, the meniscus adjustment was forced to occur within the pores of a sintered glass (category A, the largest porosity available), thus converting directly into heat the excess energy of the interface and dumping immediately all generated kinetic energy. However, to maintain the free interface condition between fluids, the circular sintered glass, fitted to the tube, was hollowed at its center. The ring thus obtained was found to be the most effective when its radial thickness was of the size of the meniscus. The water pouring process, to set up the fluid/water interface, is a delicate operation requiring the utmost care to let the water slowly drain down the glass walls to the fluid surface. In some cases, penetration of the water into the fluid was still observed. A simple rejection technique, described in section 2.5, was used to discard these experiments.

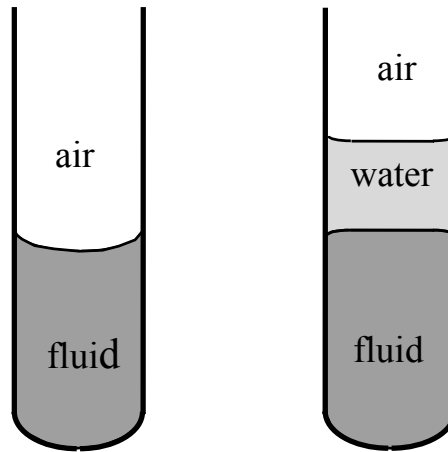


Figure 3: Meniscus on Glass Surface

The glass tubes have been specifically designed by AMIL for the testing, see Figure 4. Two temperatures were tested: close to 0°C and at room temperature. It was found ineffective to use the same tubes for both temperatures, therefore a total of 14 tubes were manufactured in two series A and B. Among the seven tubes prepared for each series, the one showing the poorest calibration results was

discarded (tubes 2A and 4B) leaving six tubes for a given experiment. The overall glass tube set-up is presented in Figure 5.

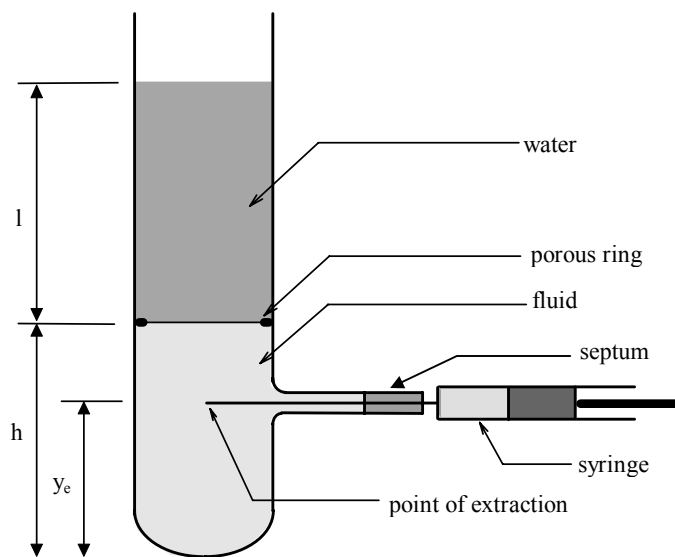


Figure 4: Water Diffusion Measurement Apparatus

A 0.1 mL syringe is introduced through the septum so that its tip is at the extraction point located at height y_e . Then, a 5 mL syringe, graduated every 0.1 mL, is used to put the fluid into the tube to the height h . Another 5 mL syringe is used to put a height l of water on top of the fluid. All tubes and syringes are thoroughly cleaned, using water and acetone, and dried before each experiment. Typically, the height values are 3 cm for h , 4 cm for l , and 1.75 cm for y_e . The volume of fluid is 4.00 mL. Errors in h and l height values due to volume measurements are about $\pm 1\%$.



Figure 5: Glass Tube Set-up

3.3 Experimental Procedure

A typical experiment is performed simultaneously with six test tubes in the same condition for the same fluid concentration ; therefore twelve tubes were thus used, six at room temperature and six in a cold chamber at 4°C. The fluid refractive index is measured just moments prior to the fluid introduction into the test tube in order to account for small concentration variations due to fluid evaporation since its dilution. All tubes and syringes are rinsed with demineralized water and dried with acetone. The experimentation set up for a given tube is performed according to the following step-by-step procedure.

- 1 - Set the tube perpendicularly on a stationary stand.
- 2 - Seal the lateral part of the tube with a rubber septum, then introduce a 0.1 mL syringe through the septum until the tip of the needle reaches the extraction point.

3 - Inject the specified fluid volume with a 5 mL syringe to the bottom of the tube until the height of the fluid reaches the sintered glass ring.

4 - Slowly inject the water above the surface of the fluid with another 5 mL syringe set along the inside wall of the tube until the water height is about 1.5 to 2 cm higher than the height of the fluid.

5 - Extract the fluid sample from the inserted syringe after a prescribed period of time (30 to 48 hours).

3.4 Concentration Measurement Method

The *neat* fluid is the product as delivered by the manufacturer. Water is initially present in the *neat* fluid. To follow the usual practice of the industry, the concentration variable definition is based on the *neat* fluid, which means that the initial fluid is a 100% concentration. Typically, manufacturers present data in weight concentration, while the users, airline companies, tend to work in terms of volume concentration. In this study, the weight concentration in neat fluid was selected to represent the level of dilution at a given point. It is thus defined as the ratio of the weight of *neat* fluid over the total fluid weight (sum of the neat fluid and the water). Throughout the text, unless otherwise specified, it will be simply referred to as the concentration, denoted C . It should be noted that weight water concentration is not equal to $(1 - C)$ since the neat fluid, i.e. the 100% concentration, may contain 20% to 50% of water, and therefore, a 50% dilution for example may correspond to up to a 75% concentration in water.

Measurement of the concentration can be performed by various methods. Unfortunately, the non-intrusive methods such as infra red absorption, which were attempted, are not precise enough, in particular for the calibrating fluid EG. Therefore, it was decided to use an extraction method in conjunction with a concentration measurement technique which would require only a minute amount of fluid to keep a good resolution in the position value y_e . Refractive index is a property which is conveniently related to the fluid concentration and can be

measured with a small amount of sample (about 0.1 mL). Moreover, this property measurement is part of the required evaluation in the laboratory certification.

A calibration curve is prepared for each fluid by measuring the values of the refractive index at different concentrations. A polynomial curve-fitting of degree 1, 2 or 3 was obtained for each fluid as defined in Equation 3, i being the refractive index. A typical calibration curve is presented in Figure 6 (EG), curve-fit coefficients for EG and PG are given in Table 1.

$$C = a_3 i^3 + a_2 i^2 + a_1 i + a_0$$

Equation 3: Polynomial Expression of Concentration

Table 1: Refractive Index Curve-fit for Ethylene Glycol and Propylene Glycol

Fluid \ coef.	a_3	a_2	a_1	a_0	R^2
EG	0	951.37	-1639.79	498.64	0.9999
PG	45986	-188580	258649	-118615	1.0000

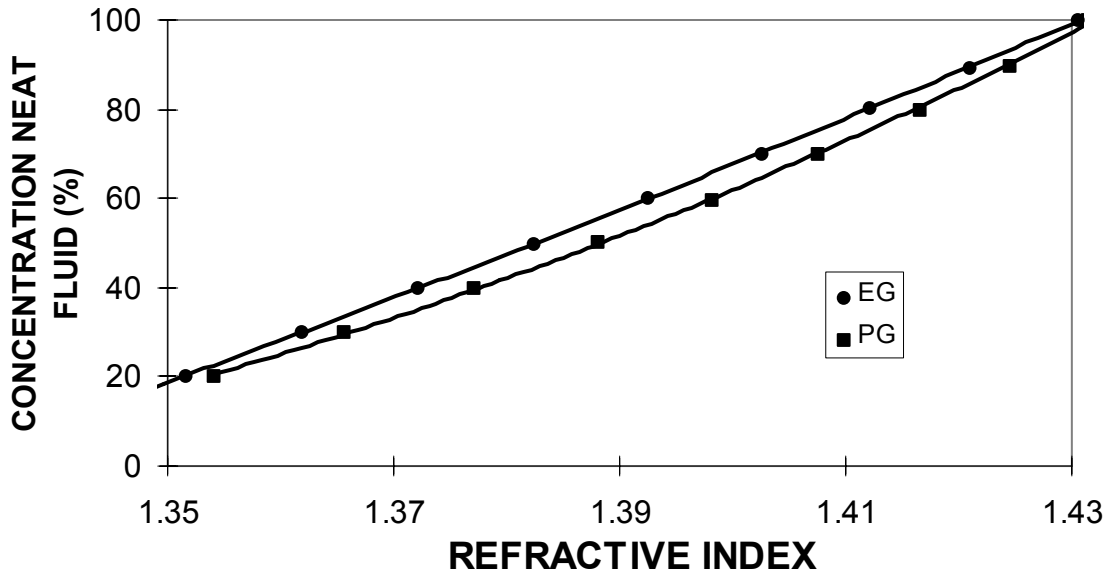


Figure 6: Ethylene and Propylene Glycol Concentration vs Refractive Index

The sensitivity of the refractive index apparatus, an ABBE-3L refractometer, is about ± 0.0002 . According to Figure 6, a 0.0001 refractive index value corresponds to a 0.1% concentration value. This relation is about the same for all fluids. This permits estimation of the relative error incurred in the water diffusion calculation by the accuracy of the refractive index measurement. For a diffusion experiment lasting long enough to generate a 5% decrease of concentration at the extraction point at the end of the test, the measured decrease in refractive index value would be 0.0050, which corresponds to a relative error of $\pm 4\%$ in refractive index and thus in water diffusion.

The value of the coefficient of diffusion calculated from the measurement at the end of the test will be attributed to the concentration averaged on the initial and final concentration. Considering that the decrease of concentration in the experiment is 5%, there will be a $\pm 2.5\%$ error in the prescribed concentration value for the test, the error in water diffusion is acceptable. For instance, if the fluid concentration was 80% at the beginning of the test and 75% at the end, the

diffusion coefficient will be considered to correspond to a $82.5 \pm 2.5\%$ fluid concentration. If we wanted to reduce the water diffusion error from 4% to 2%, then the experiment would have to be prolonged to obtain a total concentration decrease at the extraction point of 10%, yielding a $\pm 5\%$ error in the corresponding fluid concentration. There is an unavoidable trade-off error between concentration and water diffusion values.

The time period required to obtain significant diffusion at the extraction point was generally about 30 hours at room temperature and 40 hours at cold temperature.

3.5 Diffusion Calculation Method

As mentioned previously, the measured concentration value at the extraction point is to be compared to a mathematical prediction derived from the solution of an analytical model of the diffusion process taking place in the tube. Neglecting the lateral wall effects, the situation can be considered as a case of one-dimensional binary diffusion along the y-axis. According to the Fick's second law of diffusion, this process is governed by Equation 4.

$$\frac{\partial C}{\partial t} = \frac{\partial}{\partial y} \left(D \frac{\partial C}{\partial y} \right)$$

Equation 4: Model of Diffusion Process

When the column of water is of finite length, l , by introducing the concept of reflection at a boundary, an exact analytical solution of Equation 4 can be derived. The complete expression for the concentration in the system is an infinite series of error functions or error-function complements (Crank, 1976), see Equation 5,

$$C(y, t) = \frac{C_0}{2} \sum_{n=-\infty}^{n=+\infty} \left\{ \operatorname{erf} \left(\frac{h + 2nl - y}{2\sqrt{Dt}} \right) + \operatorname{erf} \left(\frac{h - 2nl + y}{2\sqrt{Dt}} \right) \right\}$$

Equation 5: Analytical Solution of Diffusion Model

where h (m) is the height of the column of the fluid, l (m), the height of the column of the water, D (m²/s), the coefficient of diffusion of the fluid, t (s), the duration of the diffusion process, y (m), the vertical coordinate, C_0 (%) the initial concentration of the fluid and C (%), the final concentration of the fluid at y and t .

Using a 40 terms truncation of Equation 5, averaged over an interval of height of ± 0.10 cm centered at $y = y_e$, and given the measured concentration C at time t , a root-finding computer program calculates the corresponding D value. Various numerical simulations indicated a marked sensitivity of the result, about 0.4×10^{-6} cm/s, in relation with the distance between the extraction point and the fluid/water interface. Considering the uncertainty related to the assessment of the position of the interface and the bottom plane, the value of the height of fluid at the extraction point, y_e , was calibrated according to a procedure described in the next section.

3.6 Calibration of the Method

The value y_e was calculated by measuring the known D value of a reference fluid with the present procedure. An iterative numerical procedure based on Equation 5 adjusts y_e to match the measured D value with its known value. In this fashion y_e is considered as a calibration factor to be determined for each tube which accounts for all discrepancies with respect to the perfect one dimensional diffusion process. The 50% concentration of EG at room temperature was chosen as reference data since EG is the only pertinent fluid for which approximate data is available and the 50% concentration was found to be the most repetitive experiment. The reference value at room temperature was taken as 6.00×10^{-6} cm²/s, which is the value inferred by extrapolation at 23°C of Byers & King data

and within 10% of their result at 25°C, see Figure 7. This choice also yielded y_e values around 1.80 cm, which are consistent with the geometrical values.

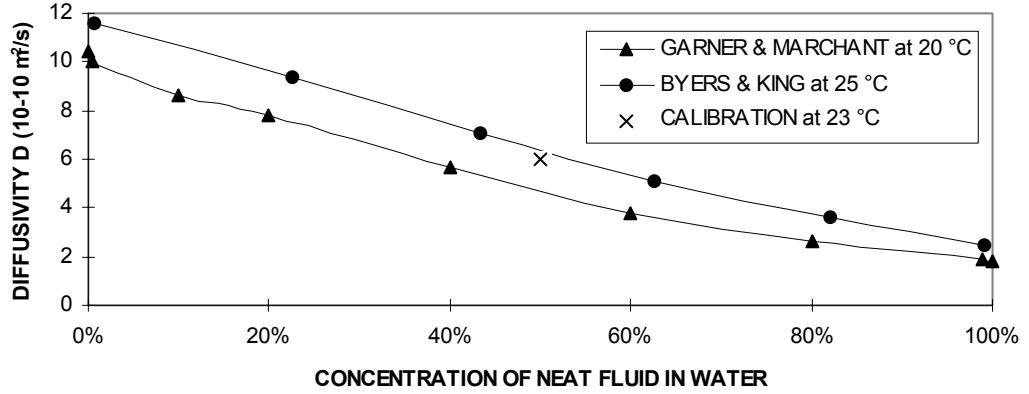


Figure 7: Calibration of Diffusion with Ethylene Glycol

The calibrated y_e values for the fourteen tubes manufactured for this study are presented in Table 2 and Table 3. The values presented in these tables, and used in subsequent experiments, are averages over calibration experiments repeated three to five times. Calibration variations were of the order of ± 0.02 cm, the related error in D value can be neglected since it corresponds to D variations of the order of $\pm 0.008 \cdot 10^{-6} \text{ cm}^2/\text{s}$. Tubes 2A and 4B presented the largest calibration variations and therefore were not used.

Table 2: Series A Tubes Calibration

tube #	1A	2A	3A	4A	5A	6A	7A
y_e (cm)	1.75	-	1.72	1.92	1.73	1.95	1.72

Table 3: Series B Tubes Calibration

tube #	1B	2B	3B	4B	5B	6B	7B
y_e (cm)	1.85	1.74	1.78	-	1.92	1.75	1.63

For a given fluid, at a given concentration and a given temperature, six experiments were performed with six different tubes. For each tube, the D value is computed according to the calculation procedure outlined in section 2.4. Among these values, the highest and lowest values are discarded and the reported result is obtained from the average over the remaining four values.

3.7 Validation of the Method

Validation of the overall method was performed by measuring the 75% concentration of EG at room temperature since it is a significant difference with a 50% concentration, and Byers & King data can be used as reference for comparison. The detailed data for the six related 48 hour experiments are presented in Table 4. According to the standard statistical rejection technique mentioned in section 2.5, results in tube 4 and 7 (*) are discarded. The result of AMIL method with EG 75%-water system ($4.16 \times 10^{-6} \text{ cm}^2/\text{s}$) is in good agreement with that of Byers ($3.83 \times 10^{-6} \text{ cm}^2/\text{s}$). This indicates a good validation in the 75% to 50% initial dilution range which is the most significant for de-icing and anti-icing fluids.

Table 4: Validation Experiments with Ethylene Glycol (75% at 23°C)

tube #	h (cm)	l (cm)	init. i (-)	final i (-)	init. C	final (%)	D (cm^2/s)
1	3.50	4.60	1.4080	1.4049	75.87	72.66	4.20
3	3.50	4.60	1.4080	1.4052	75.87	72.97	4.11
4	3.50	4.60	1.4080	1.4032	75.87	70.91	4.46*
5	3.50	4.60	1.4080	1.4050	75.87	72.76	4.22
6	3.50	4.60	1.4080	1.4035	75.87	71.22	4.11
7	3.50	4.60	1.4080	1.4055	75.87	73.28	3.88*

Further evaluation of the validity of the method can be derived from the comparison of results for EG at all concentrations with data from Byers & King as well as from Garner & Marchant adjusted to the same temperatures using the parameter R_m (Table 5). Garner & Marchant's data, shown to scale the difference between methods, are found to be consistently 15% lower than those of Byers. AMIL data with respect to Byers' results are higher for concentrations above 50% and lower for concentrations below 50% and, of course, they match at 50% since AMIL method has been calibrated against the 50% value in Byers' data adjusted at 23°C. Differences between AMIL and Byers' results are generally between 10% and 20%, with the exception of results at 100% concentration with about 30% difference. This indicates that the method is fairly accurate for this type of measurement. The larger difference at 100% does not significantly reduce the reliability of the method for de-icing and anti-icing fluids, since in concentrated form, these products generally exhibit glycol concentration between 50% and 90% and dilution due to precipitation will further decrease the concentration.

Table 5: Diffusion Coefficient for Ethylene Glycol

Temperature (°C)	Glycol Concentration (%)	Byers (adjust.) ($10^{-6} \text{ cm}^2/\text{s}$)	Garner (adjust.) ($10^{-6} \text{ cm}^2/\text{s}$)	Present ($10^{-6} \text{ cm}^2/\text{s}$)
23	100	2.16	2.07	3.22
23	75	3.83	3.31	4.16
23	50	5.96	5.21	6.00
23	25	8.47	7.79	7.08
4	100	0.87	0.84	1.38
4	75	1.70	1.47	2.22
4	50	2.89	2.53	3.14
4	25	4.50	4.14	3.91

Results for PG, shown in Table 6 for 50% and 25% concentrations, also agree well with adjusted data of Garner & Marchant (R_m was obtained by regression on data at 20°C, 25°C and 30°C).

Table 6: Diffusion Coefficient for Propylene Glycol

Temperature (°C)	Glycol Concentration (%)	Garner (adjust.) (10^{-6} cm ² /s)	Present (10^{-6} cm ² /s)
23	50	3.22	4.52
23	25	5.97	5.60
4	50	1.18	1.65
4	25	2.68	2.86

4. WATER DIFFUSION RESULTS AND DISCUSSION

4.1 Tested De-icing and Anti-icing Fluids

The fluids tested with the above described procedure were three Type I, two Type II and four Type IV fluids. Detailed formulations are proprietary and therefore cannot be disclosed. A succinct definition is indicated in Table 7. Fluids contain between 1% and 3% of additives. Some additives, particularly for Type II and Type IV fluids, are polymers which may interfere with the glycol-water interaction and modify the diffusion property of the product. Therefore, similar results would not be expected among all fluid types.

Table 7: De-icing and Anti-icing Fluid Definition

AMIL Code	Type of fluid	Glycol base	Glycol Initial Concentration Percentage
F1A	I	EG	Over 90%
F1B	I	PG	
F1C	I	PG	
F2A	II	PG	Over 55% and less than 65%
F2B	II	PG	
F4A	IV	EG	Over 50% and less than 65%
F4B	IV	PG	
F4C	IV	PG	
F4D	IV	EG	

The corresponding refractive index measurements are presented in Table 8 in the form of the regression coefficients. For all fluids the curve fit is excellent as demonstrated by the regression coefficient R^2 .

Table 8: Fluid Refractive Index Curve-fit Coefficients

Fluid \ coef.	a ₃	a ₂	a ₁	a ₀	R ²
F1A	11562	-47196	65248	-30494	1.0000
F1B	40823	-167053	228831	-104891	0.9999
F1C	40849	-167317	229385	-105220	0.9997
F2A	0	812.4	-790.8	-387.45	0.9999
F2B	0	0	1573.8	-2096.1	0.9999
F4A	0	0	1607.3	-2140.2	0.9999
F4B	0	0	1674.2	-2230.0	0.9999
F4C	0	0	1587.8	-2.114.7	0.9997
F4D	0	0	1721.5	-2293.0	0.9999

4.2 Diffusion Results

A typical example of detailed diffusion data is exhibited in Table 9. In this case, results from tube #5 and tube #6 are discarded, and D is obtained from the average value calculated over the data from the four remaining. Recorded results are $D = 0.98 \times 10^{-6} \text{ cm}^2/\text{s}$ and the observed scatter between the remaining four experiments was evaluated at $s = 0.16 \times 10^{-6} \text{ cm}^2/\text{s}$. This scatter is representative of all data and is consistent with the error assessment made in section 2.3.

Table 9: Typical Fluid Experiments Results

tube #	h (cm)	l (cm)	init. i (-)	final i (-)	init. C (%)	final C (%)	D (cm ² /s)
1B	3.00	4.10	1.4062	1.4052	73.97	72.79	0.82
2B	3.10	4.20	1.4062	1.4055	73.97	73.14	1.02
3B	3.10	4.20	1.4062	1.4056	73.97	73.26	0.91
5B	2.90	4.00	1.4062	1.4011	73.97	68.07	1.39*
6B	2.90	4.00	1.4062	1.4054	73.97	73.02	0.76*
7B	3.10	4.20	1.4062	1.4055	73.97	73.14	1.19

Diffusion results are shown in Figure 8 for Type I fluids, in Figure 9 for Type II fluids and in Figure 10 for Type IV fluids. Note that, as mentioned previously, values at high PG concentrations could not be obtained by the present columnar diffusion method due to initial disturbances generated by the large difference in free energy between PG and water interfaces.

Values are given at 4°C and at 23°C. The diffusion is considerably reduced at 4°C compared to 23°C, which will be shown in the next section to be in agreement with the proposed model.

The D values are regularly decreasing with increasing dilution. The concentrated fluids are associated systems with high hydrogen-bonded characteristics. With large solute particles, and particularly where hydrogen bonding occurs, diffusion appears to take place through a mechanism different from the movement of a molecule to a vacant site postulated in Eyring's theory (Johnson, 1956; Jost, 1965). Garner found that, in diffusion, one molecule of water is hydrogen-bonded to each hydroxyl group of propanediol (PG), and that, with higher concentrations of diol, diffusion of this chemical complex takes place, whereas with higher concentrations of water, diffusion of water molecules takes place (Garner, 1961).

Due to the large energy required to break the hydrogen bond (4.5 kcal/mol for water), it appears that, in these associated liquids, practically the whole activation energy is involved in the breaking of hydrogen bonds for the continuous diffusion of water to the fluid. This mechanism may explain the high viscosity values and the small diffusion coefficients of the fluids with high EG, PG concentrations. For low concentrations, the diffusion coefficient should tend toward the self-diffusion value of water which is $24 \times 10^{-6} \text{ cm}^2/\text{s}$.

The diffusion results for Type I and Type IV fluids seem to indicate that, with similar initial glycol content, PG based fluids exhibit slower diffusion than EG-based fluids. This is in accordance with what was found for pure EG and PG, however, no general conclusion can be inferred since the coefficients of diffusion of the fluids are much higher than those of pure EG or PG, which would suggest that the additives are also important in the diffusion process.

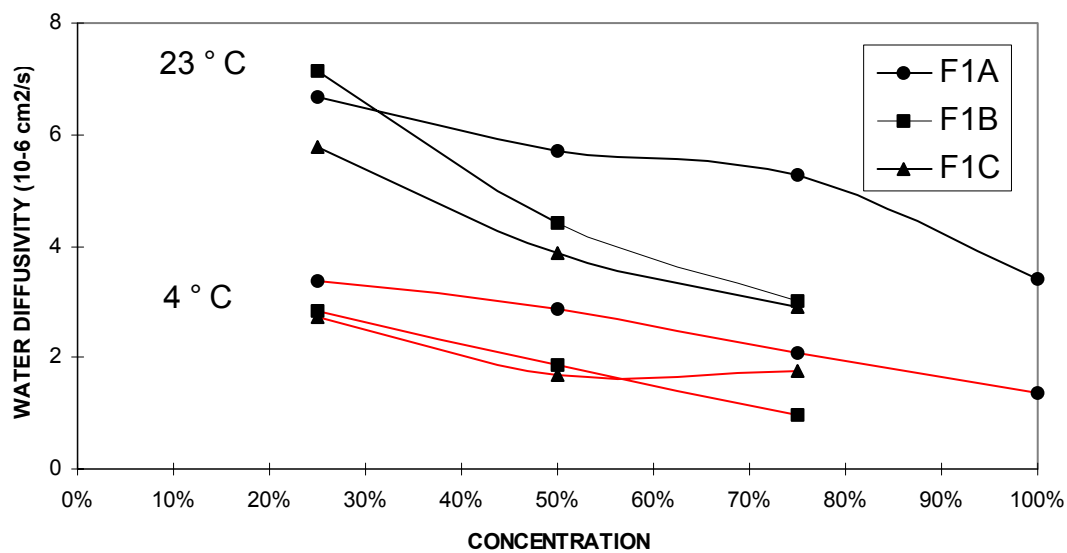


Figure 8: Type I Fluids Diffusion Coefficients

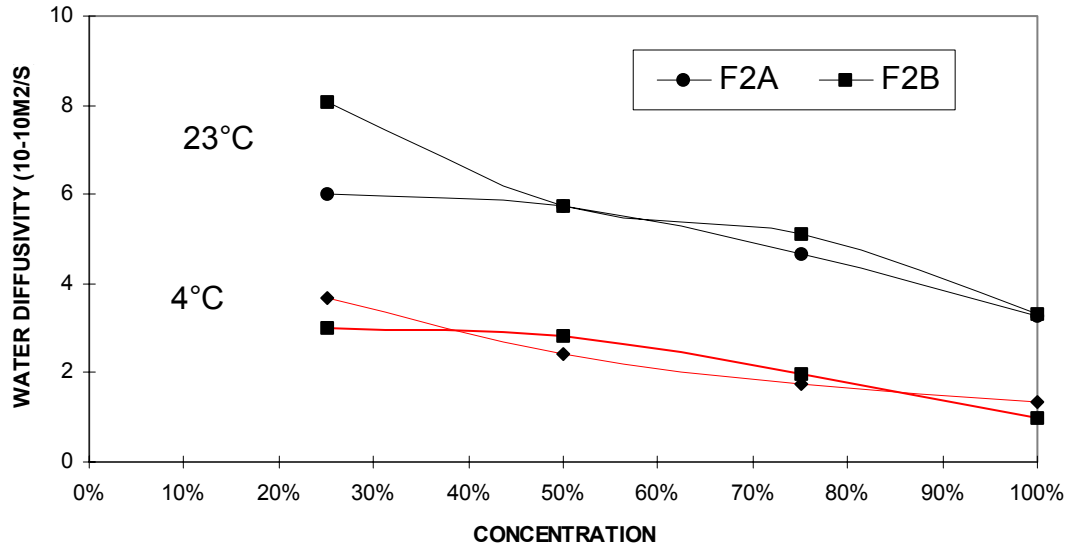


Figure 9: Type II Fluid Diffusion Coefficients

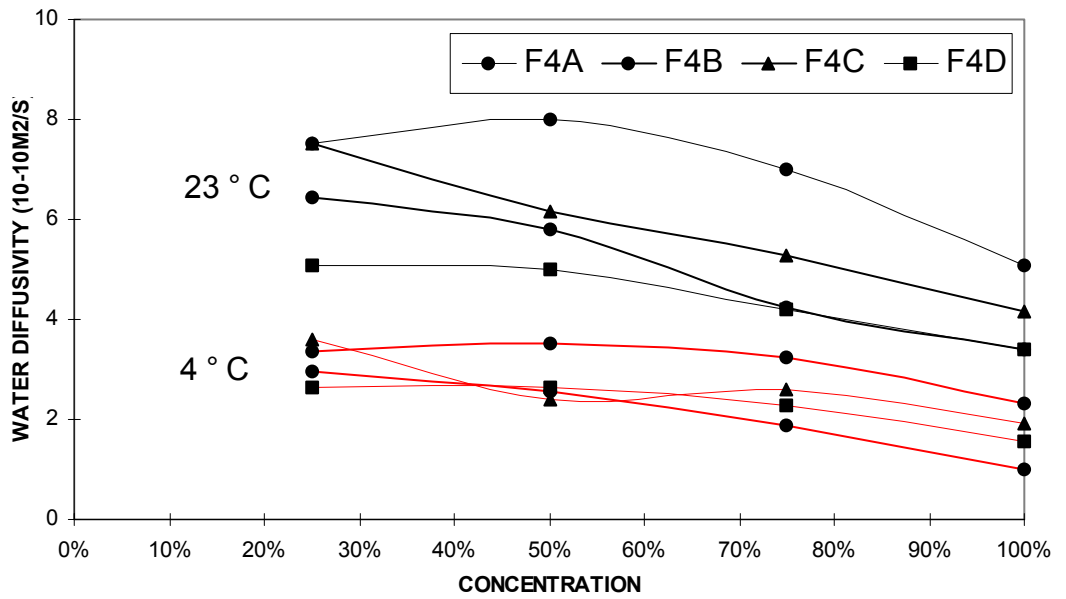


Figure 10: Type IV Fluid Diffusion Coefficients

4.3 Estimated Diffusion Coefficient and Molecular Ratio Results

The estimated diffusion coefficient, D^* , for a given fluid, is the diffusion coefficient calculated on the basis of the water and glycol content disregarding the presence of additives. The calculation at a given temperature and concentration was performed according to Equation 2 using an average R_m value in Figure 1 for EG and in Figure 2 for PG and dynamic viscosity, μ , from Curme, 1952.

The molecular ratio, which allows prediction of the temperature dependence, was calculated from Equation 2 with the help of AMIL viscosity data adjusted to the required temperature by a regression formula based on concentration, temperature and shear rate. Viscosity value at a shear rate of 0.01 s^{-1} was retained to estimate zero shear data. It should be noted that for certain fluids, significant viscosity increase can still be observed below 0.01 s^{-1} , therefore R_m values could be refined in these cases.

The estimated diffusion coefficient, D^* , and the molecular ratio, R_m , are reported in Appendix, along with measured diffusion values, D for all representative fluids listed in Table 7.

The D^* value is based on initial glycol content, about 90% in *neat* fluid for Type I fluids and about 50% for Type II and IV fluids. Results are most often quite comparable to the actual D value. However, the D^* value is sometimes slightly, but significantly, different from the actual D value. Therefore, it must be assumed that the additives are not only affecting the viscosity but also the diffusion mechanism of the water molecules.

R_m values at 23°C and 4°C , at a given concentration, are generally quite similar. Therefore the diffusion reduction is in accordance with the viscosity and temperature variation predicted by a constant R_m value.

R_m values at 50% concentration and above, for Type I fluids, are of order of 0.1, while Type II and Type IV values are of order of 0.001. It should be noted that, due to the large viscosity drop between 50% and 25% concentrations, the R_m

values at 25%, are usually much larger. This feature could complicate the derivation of an empirical formula describing R_m as a function of C . Fortunately, such a formula is only useful well above 25%, since, at -5°C (reference temperature of use) and below 25% concentration, these products are in the freezing domain (mush phase). In general R_m variation is quite smooth, exhibiting a minimum around 75% concentration, and a third order polynomial should suffice to represent this function.

The use of the molecular ratio is primarily to infer diffusion values in the cold temperature range where the fluids are used. However, it is also used to extrapolate the D value at shear rates produced by the viscous flow of the fluid along inclined surfaces such as the upper wing area of aircraft or the 10 degrees plates in the international standard certification tests. In such occurrences the maximum shear rates have been calculated at about 0.1 s^{-1} (Louchez, 1996). Consequently, viscosity can be reduced by a factor of 5 to 10 for pseudo-plastic fluids, which, according to the constant R_m value, would yield D values 5 to 10 times higher than at zero shear. Direct confirmation of the magnitude of the diffusion coefficient in transversally sheared flow is not available at this point, however numerical simulation, described in section 5, tends to indicate that, at least for small shearing as experienced in the slow draining of the fluid on aircraft body at rest, the water diffusion is well estimated by assuming a constant R_m value.

5. NUMERICAL SIMULATION

5.1 Descriptions of WSET and HHET Simulations

The experimental WSET and HHET are performed in a climatic chamber. A candidate fluid is applied on the standard inclined plates. The required precipitation is turned on after an initial five-minute delay to allow the fluid to reach a stable thickness. The time when ice, forming from the top of the plate, has progressed 25 mm (one inch) down the plate is recorded as the standard holdover time (HOT) for the test. The "one inch" criterion was found to be a good reproductive value since the time of formation of the first ice crystals is usually erratic due to the stochastic nature of the nucleation process. The corresponding analytical model has been described in detail elsewhere (Louchez 1996). The calculation domain, which is restricted to the fluid medium, is a two-dimensional geometry bounded by the solid surface of the plate and the air/fluid interface. The dimensional variables are the distance along the plate, x , and the height normal to the plate, y , see Figure 11.

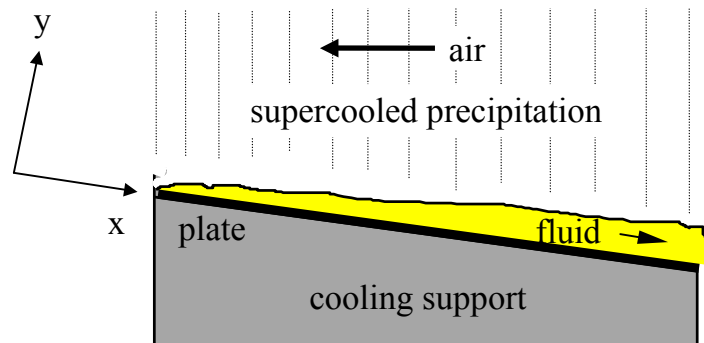


Figure 11: Problem Schematics

5.2 Governing Equations

In the model, the descriptive variables are reduced to the velocity component in the direction along the plate surface, U , the initial fluid volume concentration, C and the fluid thickness in the direction perpendicular to the plate surface, h . The governing equations are reduced to their simplest form, generally acknowledging that inertia terms are small. Temperature is considered uniform since air and plate temperature are equal (-5°C) and all heat sources such as latent heat of mixing and freezing are readily absorbed by the refrigerated plates. Fluid properties are D , the water coefficient of diffusion (m^2/s); μ , the dynamic viscosity ($\text{Pa}\cdot\text{s}$); ρ , the density (kg/m^3) and σ , the surface tension (N/m).

$$\frac{\partial U}{\partial t} = \frac{\partial}{\partial y} \left(\frac{\mu}{\rho} \frac{\partial U}{\partial y} \right) + g \sin \theta - g \cos \theta \frac{\partial h}{\partial x} + \frac{\sigma}{\rho} \frac{\partial^3 h}{\partial x^3}$$

Equation 6: Streamwise Velocity Time Evolution

$$\frac{\partial C}{\partial t} + U \frac{\partial C}{\partial x} = \frac{\partial}{\partial y} \left(D \frac{\partial C}{\partial y} \right)$$

Equation 7: Concentration Time Evolution

$$\frac{\partial h}{\partial t} = \frac{m''}{\rho_w} - \int_0^h \frac{\partial U}{\partial x} dy$$

Equation 8: Thickness Time Evolution

The other parameters appearing in these equations are the plate angle θ (deg.), the gravity acceleration g (m/s^2), the precipitation rate m'' ($\text{g/dm}^2\text{h}$) and the water density ρ_w (kg/m^3).

It should be noted that the numerical model, at low precipitation rate, can also represent the HHET situation. The impact kinetic energy can be ignored at moderate precipitation rate; it is therefore ignored in the model and, thus, there is no distinction in the modelling between the hoar-frost deposition and the impingement of supercooled (non-solid) precipitation

5.3 Calculation Strategy

The simulation starts with a uniform thickness fluid layer and a zero initial velocity according to the definition of initial state. The initial fluid thickness is taken at a value above 1 mm; this will generally reproduce the excess fluid situation prevailing in WSET. The actual initial thickness at the start of the precipitation is obtained by running the simulation without precipitation for a five-minute period of time.

The wind velocity is counted positively in the draining direction. In a typical WSET, the velocity is upstream, i.e. negative, and of the order of 0.5 m/s.

There are various mathematical models to represent non-Newtonian behaviour, such as that exhibited by anti-icing fluids. A simple, yet quite efficient, model is the corrected power law: a three-parameter law which defines the dynamic viscosity, μ , as a function of the shear rate $\dot{\gamma}$ (Butcher and Irvine, 1990). Introducing the zero shear rate value, μ_{zs} , and μ_{ls} , the viscosity value at an arbitrary low shear rate $\dot{\gamma}_{ls}$, the formula can be written in the form of Equation 9, where n is the power factor. Note that it is still a three-parameter law, since μ_{ls} and $\dot{\gamma}_{ls}$ are not independent.

$$\mu = \mu_{zS} \left(1 + \left(\frac{\mu_{zS}}{\mu_{lS}} - 1 \right) \left(\frac{\dot{\gamma}}{\dot{\gamma}_{lS}} \right)^{1-n} \right)^{-1}$$

Equation 9: Pseudo-Plastic Viscosity Law

When $n = 1$, the low shear value μ_{lS} corresponds to the constant Newtonian law value. For non-Newtonian cases, the zero shear value, μ_{zS} , cannot be experimentally measured, therefore an approximation strategy is required. The shear thinning part is reduced to a two-parameter law, which enables adequate evaluation with a reasonable number of points for curve-fitting. Using again an arbitrary $\dot{\gamma}_{lS}$, typically the lowest measured shear rate value, the result can be written in the form of Equation 10. Beyond $\dot{\gamma}_{lS}$, the viscosity is given by Equation 10. Below that value, the viscosity is assumed constant, equal to μ_{lS} .

$$\mu = \mu_{lS} \left(\frac{\dot{\gamma}}{\dot{\gamma}_{lS}} \right)^{n-1}$$

Equation 10: Reduced Pseudo-Plastic Law

The simulation runs until the freezing point is reached at some point in the fluid. Once a cell is solidified, its velocity is set at zero and its concentration is kept at freezing point value. Depending on the strategy, the calculation continues as the ice progresses down the plate. Typically the time when one inch of ice is formed is recorded for comparison with the standard experimental holdover time in WSET.

5.4 Numerical Results

Experimental results are usually given when ice has already progressed down the plate: FIE is the first icing event corresponding to the time when the one inch line is first crossed by ice and MIT is the time when the mean ice front crosses the one inch line. Considering the two-dimensional modelling, the MIT was chosen as representative of the experimental holdover time (HOT). Experimental and numerical HOT, presented in Figure 12 for WSET and in Figure 13 for HHET, are in good agreement indicating that the main features of the phenomenon are well captured by the isothermal modelling.

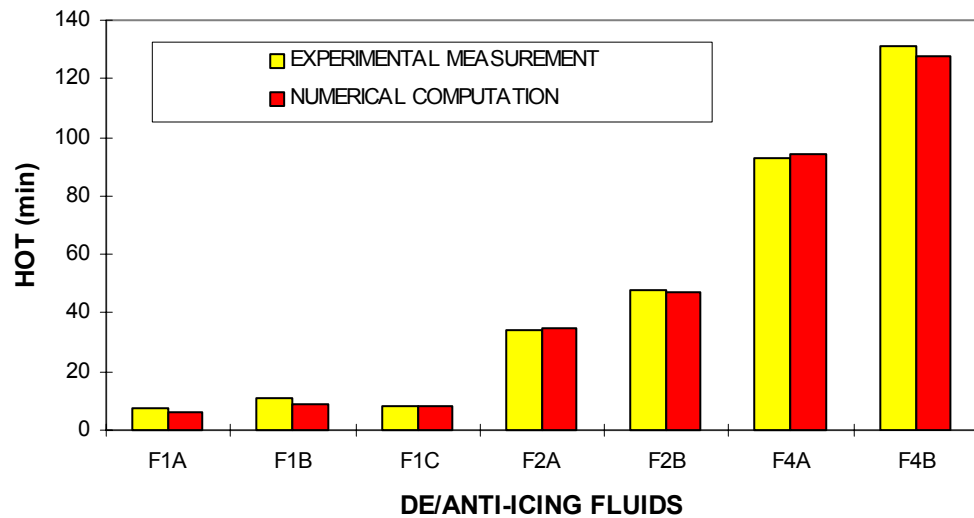


Figure 12: Validation of HOT in WSET

The role of the diffusion coefficient is important in the top layer of the fluid where it may be large enough to delay water penetration. Variations of the HOTs are shown in Figure 14 where a Type II fluid D value is arbitrarily multiplied by a factor to examine the influence of the diffusion coefficient. The time of first ice crystal appearance is also reported as FFT (first freezing time).

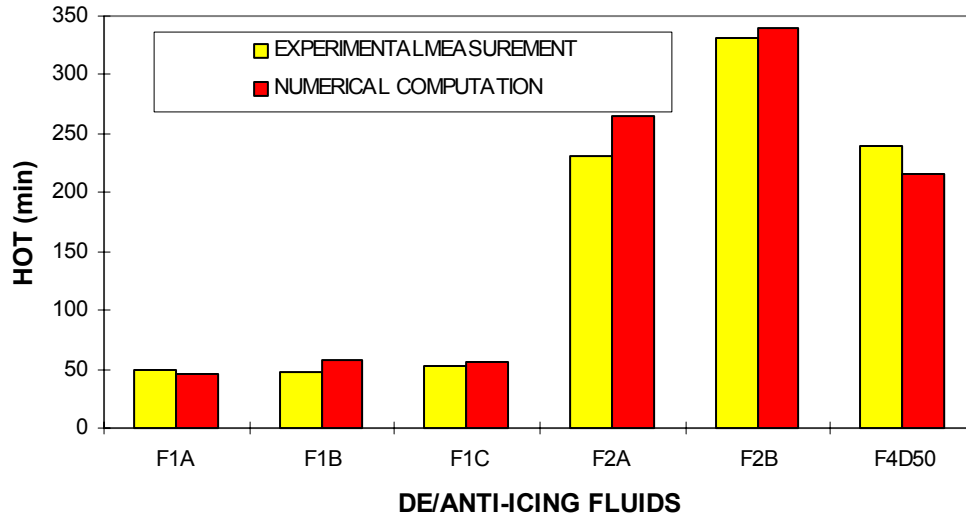


Figure 13: Validation of HET in HHET

The delay between FFT and HET indicates the time required by the ice to progress over a one inch distance down the plate. It is of order of 10 minutes.

The application of a multiplier to the actual D value is quite crude since this artificial amplification does not depend on concentration. However, the measured D value for most fluids is about reduced by half between 100% and 25% as shown in Figure 9 for Type II fluids. Therefore, a multiplication factor between 0.1 and 10 largely covers the actual D values. It can be seen that a reduction creates a increase of holdover time due to slowing of dilution in the internal fluid layers and, probably, increased draining of the highly diluted top layers. However, for a type II the reduction has to be higher than a factor of two (multiplier less than 0.5) to be significant. Clearly the role of diffusion is not very important for moderately viscous fluids such as Type II which means that the large increase in viscosity is the primary reason for Type IV effectiveness.

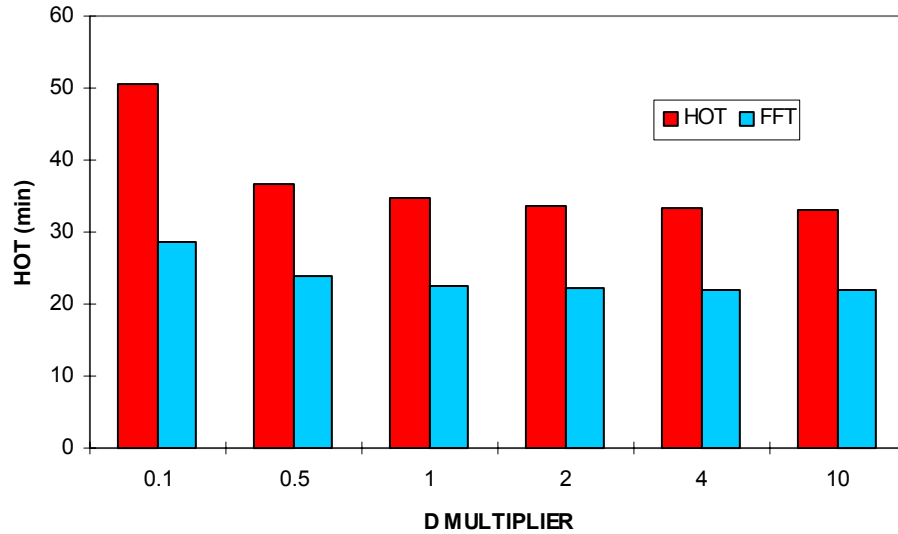


Figure 14: Water Diffusion Effect

On the other hand, just artificially increasing the viscosity on a basic Type II would not significantly improve computed HOTA. Therefore it may be surmised that it is the distinctive features of the D value of Type IV fluids which is the determining factor of improvement. However, these features are not immediately identifiable on the examination of D values in Figure 10. It is only on the molecular ratio value, R_m , at high concentration (between 75% and 100%) that a dramatic difference can be seen between Type II and Type IV. It is thus the combined effect of viscosity and diffusion which provides the resulting measured and computed increase in HOTA. Further examination of the simulation for various R_m values should help to better understand this coupled action of viscosity and diffusion.

6. CONCLUSIONS

OBJECTIVE

The objective of the experimental work was to provide a database for the determination of the diffusion coefficient of water into de-icing and anti-icing fluids at all relevant temperatures, concentrations and shear rates.

METHODOLOGY

A method was successfully developed to measure the diffusion coefficient. It is a columnar free diffusion method, using glass tubes specifically designed by AMIL for the testing. The initial concentration of the fluid and its final concentration at a fixed position in the column are determined by refractive index. The water diffusion can be calculated by the analytical solution of Fick's second law, using a 40-term truncation; given the measured concentration C at a given point and time, a root-finding computer program calculates the corresponding D value.

UTILIZATION

The calibration value was taken as $6.00 \times 10^{-6} \text{cm}^2/\text{s}$ for EG at 50% concentration at 23°C , which is the value inferred from Byers & King data. Good validation was obtained by comparison with other EG and PG data. The method exhibits a good accuracy, $\pm 5\%$, and reliability associated to a low cost design of the experimental apparatus. The method could thus be easily introduced to the manufacturers of anti-icing and de-icing fluids for the routine tests of their products.

RESULTS - DIFFUSION

Diffusion results provide values at 100%, 75% 50% and 25% concentrations at 23°C and 4°C. Values, generally found between 1 and 10 $10^{-6}\text{cm}^2/\text{s}$, increase regularly with decreasing concentration. Values are considerably reduced at 4°C compared to 23°C. This reduction was shown to be in accordance with the viscosity and temperature variation predicted by the molecular ratio, R_m , constant value. Diffusion results are close but sometimes significantly different from the coefficient of diffusion, D , value based on the glycol content only, probably as a result of the presence of large polymers, which strongly interfere with the molecular diffusion processes in the fluid. Results indicated that the water diffusion coefficient of EG and the EG-based fluids are slightly higher than those of PG and the PG-based fluids at different concentration levels, but, since as mentioned previously the diffusion results do not correspond to the glycol content, no general conclusion on the effect of the type of glycol can be inferred.

MODEL

A model of the diffusion coefficient variation with temperature and concentration was derived on the basis of well known work, which made use of the evaluation of a dimensionless parameter, called here the molecular ratio and denoted R_m , related to the ratio of molecular sizes between solvent and solute. Processing the measurements results for EG/water and PG/water systems obtained by Garner & Marchant (1961) and Byers & King (1966), confirmed that R_m is fairly constant at a given concentration.

SOFTWARE

Software developed earlier (Louchez, 1996), reproducing the WSET and HHET laboratory evaluation procedures and using an isothermal model with a constant diffusion coefficient based on equivalent EG content, was restricted to Type I and

Type II HOT predictions. This software was upgraded by the introduction of the diffusion model. The main phenomena are now well described and the holdover time calculation correctly determines the relative effectiveness of all fluids including Type IV fluids. The deviation from experimental standard value is such that the code, at this stage of development, can provide a reliable diagnostic for fluid performance certification and, therefore, can be proposed as a complement for the cold chamber testing.

RECOMMENDATION

Considering the fact that an increasing number of HOT assessments are performed on non-refrigerated plates and at differing air and plate temperatures, it is recommended that the software development include all thermal phenomena such as the release of latent heat upon water/glycol mixing and ice formation. This thermal model is also a necessary step toward the simulation of discrete particle precipitation such as snow and freezing rain.

REFERENCES

1. Aerospace Material Specifications AMS 1424 (1993). "De/Anti-Icing Fluid, Aircraft, Newtonian- SAE type I", January 1, 1993.
2. Aerospace Material Specification, AMS 1428 (1993). "Fluid Aircraft De-icing/Anti-icing/Non Newtonian, Pseudo-Plastic, SAE Type II", January 1, 1993.
3. Aerospace Materials Specification, AMS 1428B (1997). "De/Anti-icing Fluid - SAE Type II, Type III and Type IV", currently under revision.
4. Butcher, T.A. and Irvine, T.F., (1990). "Use of the Falling Ball Viscometer to Obtain Flow Curves for Inelastic, Non-Newtonian Fluids". Journal of Non-Newtonian Fluid Mechanics, 36, 1990, pp. 51-70.
5. Byers, C.H. and King, C.J., (1966). "Liquid diffusivities in the glycol-water system" The journal of physical chemistry. Vol. 70, pp. 2499-2503.
6. Crank, J., (1976). "The mathematics of diffusion" Brunel University Uxbridge Clarendon Press Oxford. pp. 1-17.
7. Curme, G.O. and Johnston, F., (1952). "Glycols" Reinhold Publishing Corporation. New York. pp. 27-57, pp. 210-232.
8. Einstein, A. (1905). Ann. Physik[4] 17, p. 549.
9. Garner, F.H. and Marchant, P.J.M., (1961). "Diffusivities of associated compounds in water" TRANS.INSTNCHEM.ENGRS. Vol. 39, pp. 397-408.
10. Hung, D.M., (1976). "Interferometric determination of diffusion coefficients, binary liquid mixtures near their critical mixing point" Ph.D. thesis of University of Quebec at Montreal.
11. Johnson, P.A. and Babb, A.L., (1956). "Liquid diffusion of non-electrolytes" Chemical reviews. Vol. 56, pp. 388-403.
12. Jost, W., (1965). "Diffusion in solids, liquids, gases" Academic Press Inc., Publishers New York. pp. 32-45.

13. Laforte, J.L., Louchez, P.R., Bouchard, G. and Ma, F., (1990). “A facility to evaluate performance of aircraft ground de/anti-icing” Cold Regions Sciences Technology. Vol. 18, pp. 161-171.
14. Laforte, J.L., Louchez, P.R., and Bouchard, G. (1992). “Cold and humid environment simulation for de/anti-icing fluids evaluation” Cold Regions Sciences Technology. Vol. 20, pp. 195-206.
15. Louchez, P.R., Laforte, J.L. and Bouchard, G. (1996). “Analysis of Ground Aircraft De/Anti-Icing Fluid Laboratory Holdover Time and Physical Properties” Prepared for the Dryden Commission Implementation Program, Transport Canada, Report TP12712E, March 1996, 111pp.
16. Tyrrell, H.J.V., (1961). “Diffusion and heat flow in liquids” London Butterworths. pp. 75-122.
17. Sherwood, T.K., Pigford, R.T. and Wilke, C.R. (1975). “Mass Transfer” McGraw-Hill.

APPENDIX A:
FLUID PROPERTIES

The following tables provide the measured diffusion coefficient D (in m^2/s) for three Type I fluids, coded F1A, F1B and F1C, two Type II fluids, coded F2A and F 2B, and four Type IV fluids, coded F4A, F4B, F4C and F4D. Values have been measured at two temperatures, 4°C and 23°C , and at four fluid weight concentrations 100%, 75%, 50% and 25%. Also reported are the estimated diffusion coefficient D^* (in m^2/s) calculated on the basis of the glycol content disregarding the presence of additives in the fluid. Finally, the molecular ratio R_m calculated from the D value, the zero shear dynamic viscosity μ (in $\text{Pa}\cdot\text{s}$) and the temperature T (in K) is also given.

T ($^\circ\text{C}$)	C (%)	D ($10^{-6} \text{ cm}^2/\text{s}$)	D* ($10^{-6} \text{ cm}^2/\text{s}$)	Rm
23	25	6.67	8.64	3.20
23	50	5.72	6.26	0.33
23	75	5.28	4.21	0.13
23	100	3.42	2.55	0.33
4	25	3.36	4.43	2.04
4	50	2.88	2.94	0.32
4	75	2.07	1.81	0.16
4	100	1.36	1.00	0.24

Table-Appendix 1: Diffusion Coefficients for F1A

T (°C)	C (%)	D (10^{-6} cm ² /s)	D* (10^{-6} cm ² /s)	Rm
23	25	7.15	6.27	2.42
23	50	4.42	3.62	0.62
23	75	3.02	1.95	0.28
4	25	2.83	2.91	1.25
4	50	1.85	1.33	0.44
4	75	0.98	0.62	0.26

Table-Appendix 2: Diffusion Coefficients for F1B

T (°C)	C (%)	D (10^{-6} cm ² /s)	D* (10^{-6} cm ² /s)	Rm
23	25	5.78	6.22	3.08
23	50	3.88	3.55	0.27
23	75	2.91	1.89	0.29
4	25	2.71	2.88	1.23
4	50	1.68	1.30	0.25
4	75	1.76	0.60	0.16

Table-Appendix 3: Diffusion Coefficients for F1C

T (°C)	C (%)	D (10^{-6} cm ² /s)	D* (10^{-6} cm ² /s)	Rm (10^{-3})
23	25	6.03	7.29	1.72
23	50	5.72	5.17	1.91
23	75	4.67	3.49	1.55
23	100	3.28	2.29	0.92
4	25	3.84	3.61	2.58
4	50	2.44	2.20	1.95
4	75	1.74	1.27	2.10
4	100	1.34	0.74	3.22

Table-Appendix 4: Diffusion Coefficients for F2A

T (°C)	C (%)	D (10^{-6} cm ² /s)	D* (10^{-6} cm ² /s)	Rm (10^{-3})
23	25	8.06	7.54	6.17
23	50	5.75	5.57	0.59
23	75	5.09	3.97	0.25
23	100	3.30	2.74	0.83
4	25	3.00	3.78	3.46
4	50	2.82	2.45	0.61
4	75	1.97	1.51	0.65
4	100	0.99	0.92	4.31

Table-Appendix 5: Diffusion Coefficients for F2B

T (°C)	C (%)	D (10^{-6} cm ² /s)	D* (10^{-6} cm ² /s)	Rm (10^{-3})
23	25	7.52	9.51	13.82
23	50	8.00	7.89	0.20
23	75	7.01	6.36	0.03
23	100	5.07	4.97	0.07
4	25	3.38	5.04	9.63
4	50	3.53	3.94	0.21
4	75	3.26	3.00	0.04
4	100	2.31	2.21	0.07

Table-Appendix 6: Diffusion Coefficients for F4A

T (°C)	C (%)	D (10^{-6} cm ² /s)	D* (10^{-6} cm ² /s)	Rm (10^{-3})
23	25	6.44	7.73	0.24
23	50	5.80	5.90	0.03
23	75	4.24	4.36	0.03
23	100	3.41	3.14	0.18
4	25	2.96	3.92	0.42
4	50	2.56	2.66	0.05
4	75	1.88	1.72	0.05
4	100	1.00	1.10	0.41

Table-Appendix 7: Diffusion Coefficients for F4B

T (°C)	C (%)	D (10^{-6} cm ² /s)	D* (10^{-6} cm ² /s)	Rm (10^{-3})
23	25	7.51	9.46	0.75
23	50	6.16	7.79	0.07
23	75	5.28	6.22	0.03
23	100	4.18	4.79	0.04
4	25	3.59	5.00	4.41
4	50	2.39	3.87	0.33
4	75	2.61	2.91	0.07
4	100	1.92	2.11	0.09

Table-Appendix 8: Diffusion Coefficients for F4C

T (°C)	C (%)	D (10^{-6} cm ² /s)	D* (10^{-6} cm ² /s)	Rm (10^{-3})
23	25	5.08	7.69	0.62
23	50	4.98	5.83	0.13
23	75	4.21	4.28	0.06
23	100	3.41	3.05	0.07
4	25	2.65	3.89	2.28
4	50	2.66	2.62	0.19
4	75	2.27	1.67	0.10
4	100	1.55	1.06	0.38

Table-Appendix 9: Diffusion Coefficients for F4D